Quantifying lipids in human cells using Raman spectroscopy

Barbara Orzechowska[1], Anna Nowakowska[1], Anna Pieczara[1], Wiktoria Korona[1,2], Łukasz Mateuszuk[3], Malgorzata. Baranska[1,*]

[1]Jagiellonian University, Faculty of Chemistry, Gronostajowa 2, 30-387, Krakow, Poland,
[2]Jagiellonian University in Krakow, Doctoral School of Exact and Natural Sciences, Lojasiewicza 11, Krakow, Poland
[3]Jagiellonian University, Jagiellonian Centre for Experimental Therapeutics (JCET), Bobrzynskiego 14, 30-348 Krakow, Poland

Corresponding author: Malgorzata Baranska, m.baranska@uj.edu.pl

Abstract

Omics methods should deliver information on cellular composition as well as their content and localization in cells. This is particularly important for lipids, both saturated and unsaturated fatty acids, which regulate key metabolic, signaling, and toxic processes. Furthermore, differences in local concentration can determine cell fate: activating endoplasmic reticulum stress, exacerbating lipotoxicity, or promoting metabolic adaptation. By using deuterated fatty acids as Raman probes (Rp), we can determine their local concentrations within cells, taking into account, for example, accumulation in lipid droplets, ER or membranes. Monitoring the incubation time and distribution of Rp allows for the assessment of the rate of lipid uptake and accumulation in the cell. Therefore, Raman microscopy (RM) methods can be used to study the kinetics of lipid transport and metabolism, key in fluxomics. We quantitatively calibrate the C–D band intensities using deuterated lipid standards and compare the RM results with Liquid Chromatography–Mass Spectrometry (LC-MS) and Fluorescence Microscopy (FM) data to verify the quantitative accuracy of the Raman method. We demonstrate that despite using μM concentrations of deuterated Palmitic Acid (dPA) and deuterated Oleic Acid (dOA) in the medium, local concentrations inside cells (especially in lipid droplets) can reach mM levels which demonstrates the importance of a local, not just total, lipid detection method.

Introduction

Analysis of local metabolite concentrations is a key metabolic and functional parameter, and high local concentrations are crucial for biological function and effects. Application in lipotoxicity studies (high local concentrations of saturated fatty acids lead to activation of Endoplasmic Reticulum (ER) stress, PERK/eIF2α, autophagy, and even apoptosis), by localizing them, one can predict cell susceptibility to death induced by high local lipid concentrations. [1] Tracking cancer metabolism, where cells strongly alter lipid metabolism by synthesizing fatty acids de novo or utilizing exogenous ones, can also be explored.[2] Cell preference for saturated or unsaturated fatty acid accumulation can be considered a marker of the cancer phenotype.[3,4] The location and concentration of fatty acids can help in the selection of drugs that inhibit the elongation of fatty acid carbon chains, their synthesis or the activation of oxidation, which allows for testing the effectiveness of treatment by monitoring the distribution of fatty acids in time and space.[5]

RM has become an increasingly powerful tool for the *in situ* analysis of lipids in biological and biomedical applications.[6–9] This technique provides chemically specific vibrational fingerprints without the need for external labels and in a non-destructive manner[10,11], enabling spatially resolved measurements of lipid composition in highly heterogeneous matrices as biological samples.[12–14] A great advantage of RM is its high temporal and spatial resolution[15], which enables subcellular chemical imaging and is particularly important for lipid biology due to the strong compositional heterogeneity of cellular compartments, membranes, and lipid droplets.[10] As interest grows in single-cell lipidomics[16], metabolic phenotyping[17], and high-resolution mapping of lipid droplets and tissues[9], (semi-)quantitative Raman analysis has emerged as a key analytical approach for characterizing the degree of fatty-acid saturation directly within intact systems.[6,18,19] A key feature that sets RM apart

from other lipidomics techniques is that it does not require lipid extraction from cells, making it suitable for *in vivo* analysis, where maintaining physiological conditions is crucial.[20] However, despite its advantages, accurate quantitative discrimination between saturated and unsaturated fatty acids remains technically challenging.

Quantitative RM relies on robust calibration and reference strategies to accurately link spectral features to lipid composition. Reliable quantification requires addressing several significant challenges, including differences in Raman cross-sections, spectral overlap, band position or shape, noise originating from instruments, samples, and external sources, and autofluorescence.[21] External calibration using fatty-acid mixtures of known composition enables the construction of calibration curves based on intensity or area ratios of characteristic vibrational bands associated with lipid unsaturation and saturation.[22] Ratiometric normalization to stable internal spectral features, such as C–C stretching (band 1006 cm^{-1}), CH_3/CH_2 scissoring (band 1440 cm^{-1}), C=C stretching (band 1660 cm^{-1}), and CH_3/CH_2 symmetric stretching (band 2930 cm^{-1}) modes, is widely employed to enhance reproducibility, assuming relatively constant lipid packing.[23] For complex and heterogeneous samples, multivariate chemometric methods, such as Partial Least-Squares Discriminant Analysis (PLS-DA), Principal Component Analysis (PCA) or spectral phasor analysis provide greater robustness by exploiting the full spectral information.[22,24,25] Raman-based quantitative analyses can be validated through comparison with orthogonal techniques such as LC–MS, Fourier Transform Infrared Spectroscopy (FTIR) or Nuclear Magnetic Resonance (NMR). Absolute, reference-free quantification is theoretically feasible under well-defined conditions but remains challenging in biological systems.

Materials and Methods

Sample preparation

HeLa (Human cervical cancer cell, Sigma Aldrich) were cultured in MEME medium (Minimum Essential Medium Eagle, Sigma-Aldrich, Merck, Darmstadt, Germany), supplemented with 5 % heat-inactivated fetal bovine serum (FBS, Lonza), 1% Penicillin-Streptomycin (Sigma-Aldrich), 1% L-Glutamine solution (Sigma-Aldrich, Merck, Darmstadt, Germany) and 1% MEM Non-essential Amino Acid Solution (Sigma-Aldrich, Merck, Darmstadt, Germany, cat. No M7145). Cell cultures were maintained at 37 °C in a 98 % air / 5 % CO_2 atmosphere and passaged every 4 to 5 days upon reaching 80 % confluence. HeLa cells were seeded onto sterilized CaF_2 slides (12 mm in diameter and 1 mm thick; Crystran, UK) at a density of 50,000 cells per well in a 24-well plate and incubated for 24 hours to adhere. On the day of treatment, the culture medium was replaced with a fresh medium. The d_{31}-Palmitic Acid (d_{31}-PA, Sigma-Aldrich, Merck, Darmstadt, Germany) solution was added directly to the medium at 200 µM and 50 µM for 6 h or 24 h of incubation. To facilitate fatty acid transport across the cell membrane, d31-PA was first saponified with NaOH (Sigma-Aldrich, Merck, Darmstadt, Germany) at 70 °C and then conjugated to bovine serum albumin (BSA, fatty acid-free, Sigma-Aldrich, Merck, Darmstadt, Germany). After incubation, cells were gently rinsed with Dulbecco's phosphate-buffered saline (DPBS; Sigma-Aldrich, Merck, Darmstadt, Germany) and fixed for 10 minutes at room temperature in 2.5% glutaraldehyde (Sigma-Aldrich, Merck, Darmstadt, Germany). The fixed cells were kept in DPBS at 4°C until measurements were taken. Just before measurements, the cells were rinsed with room-temperature DPBS.

Raman measurements of HeLA cells

Raman imaging of HeLa cells was performed using a confocal Raman microscope (WITec Alpha 300; WITec GmbH, Ulm, Germany)s, using an air-cooled solid-state laser with an excitation wavelength of 488 nm, and a CCD detector (Andor Technology Ltd., Belfast, Northern Ireland). A 488 nm excitation wavelength was used, with a laser power of approximately 50 mW measured at the objective back aperture. Data processing was conducted using WITec Project FIVE 5.2 software. Spectral preprocessing included removal of cosmic ray artifacts and baseline subtraction using a third-order polynomial.

Construction of a calibration curve for dPA concentration determination

To construct the calibration curve, dPA powder (Sigma-Aldrich, Merck, Darmstadt, Germany) was dissolved in oleic acid (Sigma-Aldrich, Merck, Darmstadt, Germany) at concentrations ranging from 0 mM up to 3.477 M. The resulting solutions were deposited onto CaF_2 slides (12 mm in diameter and 1 mm thick; Crystran, UK), chosen for their low Raman background and high optical transparency in the spectral range of interest. Raman spectra for the calibration measurements were acquired using a 488 nm excitation laser at approximately 50 mW measured before the objective. The measurements were performed using a confocal Raman microscope (WITec Alpha 300; WITec GmbH, Ulm, Germany) and a 100× dry objective. To ensure reproducibility and statistical robustness, the calibration measurements were repeated three times independently. For each concentration point, spectra were acquired from multiple locations on the CaF_2 slide to account for potential sample inhomogeneity and instrumental variability. For dPA signal intensity analysis, the C–D vibrational band was integrated in the silent region using OPUS 7.0 software (Bruker, MA, USA). Before determining the integrated values, baseline correction was performed and the spectra were normalized.

Fluorescence measurements

HeLa cells were incubated for 24 h with fluorescent palmitic acid (FM-PA) (NBD, Sigma-Aldrich, Merck, Darmstadt, Germany) at concentrations ranging from 5 µM to 100 µM, then fixed with 2.5% glutaraldehyde and stained with Hoechst (Sigma-Aldrich) and CellMask Red (Sigma-Aldrich, Merck, Darmstadt, Germany). Fluorescence measurements were subsequently performed using the Axio Observer.D1 (Zeiss, Oberkochen, Germany) fluorescence microscope.

Results

1. Single-Pixel–to–Single-Cell Quantification Strategy

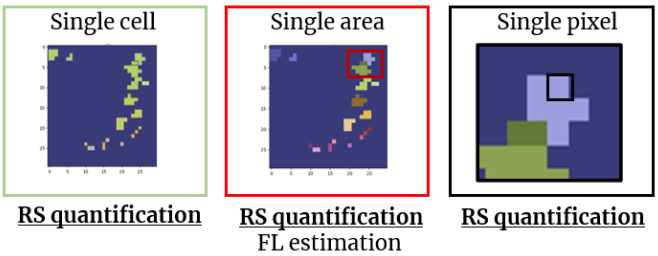

Figure 1. Three levels of quantification of deuterated fatty acids in cells.

The scheme in **Figure 1** illustrates the overall concept of multi-scale determination of deuterated fatty acid concentrations using Raman spectroscopy combined with fluorescence microscopy. This integrated approach enables quantitative analysis of probe uptake and distribution across spatial scales, ranging from the whole-cell level to subcellular regions and down to individual pixels with a size of 1 µm, thereby capturing both global and local aspects of fatty acid concentration heterogeneity. To quantitatively analyze this variability, three complementary analytical strategies were established.
The first strategy, *single-cell concentration*, focuses on estimating the average intracellular dPA concentration within an individual cell. The second strategy, *single-area concentration analysis*, combines fluorescence microscopy with RM to investigate chemically similar intracellular regions. In this approach, Raman spectra are averaged over a selected area exhibiting comparable spectral features, enabling semi-quantitative assessment of dPA distribution within specific subcellular domains. Fluorescently labeled palmitic acid is used as a reference to guide region selection and to facilitate comparison between fluorescence and Raman-derived distributions, despite the chemical differences between the probes. The third strategy, *single-pixel concentration analysis, relies* exclusively on Raman spectroscopy and enables direct quantification of dPA concentration within chemically homogeneous regions at the level of individual pixels. This method relies on chemical mapping and precise spectral classification to ensure that each pixel represents a well-defined chemical environment. By minimizing spatial averaging, this approach provides the highest spatial resolution

and the most localized concentration estimates. Concentration analysis at each level will be discussed in detail in the respective sections.

Regardless of the concentration level at which the analysis is performed, the first step in the quantitative analysis strategy is to construct a calibration curve. It is essential to convert measured Raman signal intensities into quantitative concentration values, as shown in **Figure 2**. In our studies, to prepare a calibration curve, we dissolved dPA at defined concentrations spanning a broad range, from 0 mM up to 3.477 M in oleic acid (OA). OA was chosen as a chemically relevant lipid matrix that mimics the intracellular lipid environment. This enabled coverage of both low and high signal intensities of dPA expected in cellular measurements.

Figure 2A shows the spectral range over which the dPA band was integrated in the silent region to establish the relationship between the dPA concentration in OA and the dPA signal (**Figure 2B**). As shown in the calibration curve (**Figure 2B**), the linear relationship between concentration and signal intensity was maintained over a wide range of concentrations (up to 3.477 M). A linear function, described by the equation y=142(±18)·x was fitted to the obtained relationship (R^2=0.9122) and subsequently used to determine the dPA concentration in cells at different levels, ranging from the single-cell to the single-pixel level.

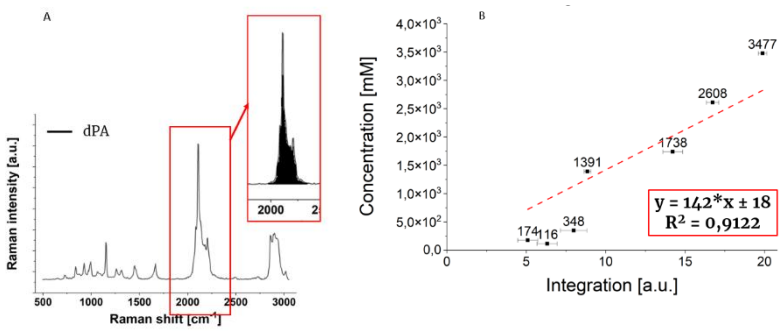

Figure 2. Construction of a calibration curve enabling dPA concentration determination from the dPA signal. (A) The schematic showing the spectral integration range of the C–D Raman band of dPA used to analyze the signal intensity of dPA. (B) The corresponding calibration curve for dPA, showing the relationship between band integrated intensity and dPA concentration dissolved in OA.

2. Determination of fatty acid concentration at the single-cell level

Figure 3 presents the results of the analysis of the single-cell intracellular concentration of dPA in HeLa cells following incubation with 50 µM and 200 µM dPA for 6 h and 24 h, illustrating the effects of both incubation time and applied dose on probe accumulation.

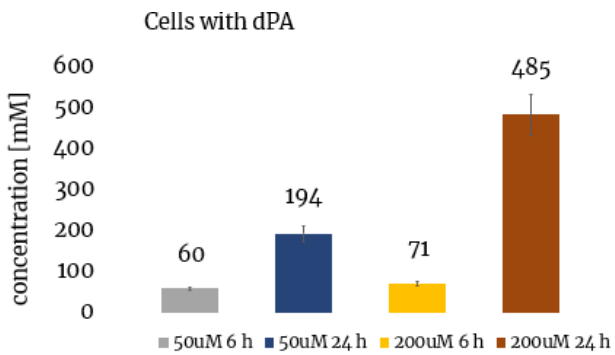

Figure 3. Single-cell level analysis of concentrations of dPA in HeLa cells incubated with 50 uM and 200 uM dPA for 6 h and 24 h.

After 6 hours of incubation of HeLA cells with dPA, the mean single-cell intracellular concentration of dPA was nearly identical for cells exposed to 50 µM and 200 µM dPA (**Figure 3**),

indicating that short incubation times result in comparable levels of probe uptake regardless of the applied extracellular concentration. This observation suggests that, at early time points, cellular uptake mechanisms may be constrained by transport capacity, likely by membrane proteins, metabolic processing, or initial partitioning into intracellular compartments, rather than by the external dPA concentration. In contrast, prolonged incubation (24 h; **Figure 3**) resulted in a pronounced increase in the mean intracellular dPA concentration. This increase was strongly dependent on the applied dPA concentration in the extracellular matrix: at the higher incubation concentration (200 µM), the mean intracellular dPA level was approximately 2.5-fold higher than that observed at the lower concentration (50 µM). These results indicate that, over time, cells continue to accumulate and metabolize dPA, resulting in increased intracellular retention of deuterated fatty acid.

Overall, extending the incubation time significantly increases intracellular dPA concentration, with this effect being substantially more pronounced at higher extracellular doses (50 µM vs 200 µM). The observed trends clearly demonstrate a combined time- and dose-dependent relationship, reflecting the interplay between uptake kinetics, intracellular storage, and metabolic incorporation of deuterated fatty acids.

3. Subcellular-level determination of fatty acid concentration

Figure 4 shows the percentage distribution of lipid droplets with varying levels of incorporated fluorescently labeled palmitic acid or deuterated fatty acid, as determined by fluorescence and Raman measurements, respectively. Lipid droplets were classified into low-, medium-, high-, and very-high-intensity groups based on signal intensity. The analysis was performed at the subcellular level for individual regions. The identified regions comprised either single lipid droplets or chemically homogeneous areas in which fatty acids were accumulated. The selected data presentation approach allowed for direct comparison of lipid droplet analyses derived from different imaging modalities.

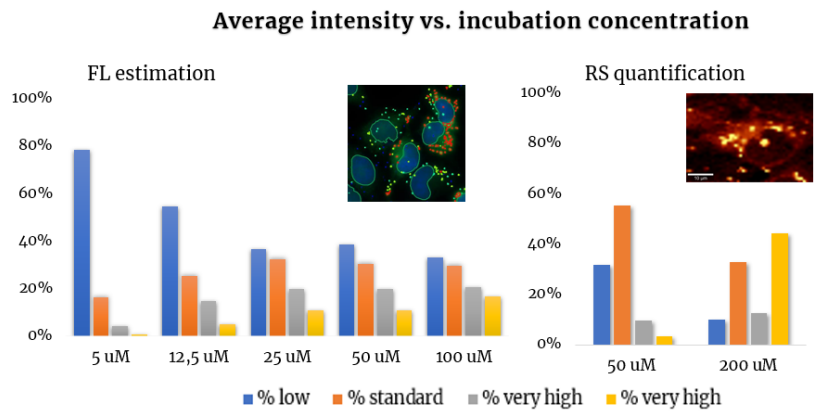

Figure 4. Subcellular-level analysis of palmitic acid accumulation obtained using complementary imaging modalities. (A) Representative fluorescence map of lipid droplets labeled with fluorescent palmitic acid (a concentration ranging from 5 µM to 100 µM), together with bar plots showing the percentage distribution of lipid droplets classified into low, medium, high, and very high signal intensity groups. (B) Representative Raman map of lipid droplets containing dPA (at concentrations of 50 µM and 200 µM) based on the C–D vibrational band, along with the corresponding bar plots showing the percentage distribution of lipid droplets across the same intensity categories.

The results presented in **Figure 4** enable comparison of the fractions of lipid droplets classified into low-, medium-, high-, and very-high-signal-intensity groups obtained using two complementary imaging methods: Raman and fluorescence microscopy. In fluorescence measurements, a pronounced decrease in the fraction of low-intensity FL-PA-rich regions is observed, accompanied by a modest increase in the fraction of regions with higher PA fluorescence intensity. This trend likely reflects increased accumulation of the fluorescent probe at higher incubation concentrations, potentially due to preferential sequestration within lipid droplets, which are major storage sites for fatty acids (**Figure 4A**). In contrast, Raman spectroscopic analysis reveals a distinctly different distribution pattern. At

lower incubation concentrations, the intracellular dPA signal is dominated by regions with intermediate C–D band intensities, indicating moderate enrichment of deuterated species throughout the cell. As the incubation concentration increases, a pronounced shift toward regions with strongly elevated deuterium signal intensities is observed. This shift indicates the formation of highly dPA-rich intracellular domains and suggests a concentration-dependent accumulation of dPA that is more uniformly detectable across multiple cellular compartments (**Figure 4B**).

s

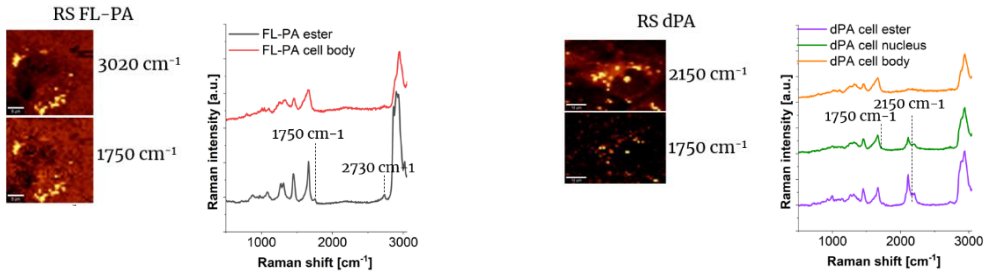

Figure 5. Raman imaging of HeLA cells incubated with (A) FL-PA and (B) dPA. (A) Chemical maps showing the distribution of unsaturated lipids (3020 cm^{-1}) and esterified lipids (1750 cm^{-1}) in cells incubated with FL-PA, with corresponding spectra of lipid droplets and cell body. (B) Chemical maps showing the distribution of dPA (2150 cm^{-1}) and esterified lipids (1750 cm^{-1}) in cells incubated with dPA, with corresponding spectra of lipid droplets, cell nucleus and cell body.

Figure 5 presents representative Raman images and corresponding spectra obtained for FM-PA and dPA in HeLa cells, illustrating the differences in spatial distribution and signal intensity between the two probes.

For cells incubated with FM-PA (**Figure 5A**), chemical Raman maps highlight the distribution of unsaturated lipids via the C=C stretching band at 3020 cm^{-1} and esterified lipids via the ester C=O stretching band at 1750 cm^{-1}, revealing a pronounced accumulation of lipid species within lipid droplets. Representative spectra extracted from lipid droplets and the cell body further confirm the lipid-rich character of these regions.

In contrast, Raman imaging of cells incubated with dPA (**Figure 5B**) enables direct visualization of the probe via the C–D vibrational band at 2150 cm^{-1}, located within the cellular silent region. The corresponding chemical maps show a distinct intracellular distribution of dPA relative to esterified lipids, with signal enrichment in lipid droplets and detectable contributions in the cell body. Spectra acquired from lipid droplets, the cell nucleus, and the cell body confirm the specificity of the dPA signal and demonstrate its suitability for subcellular-level localization and quantitative analysis.

The observed differences in the percentage distribution of regions with comparable intensities, classified into low-, medium-, high-, and very-high-signal-intensity groups, obtained by fluorescence and Raman microscopy (**Figure 4**), can be attributed to several factors.

First, FM-PA and dPA represent chemically distinct Raman probes with fundamentally different biological properties. FM-PA exhibits significantly higher cytotoxicity, which restricts its use to relatively low incubation concentrations and limits the dynamic range of achievable intracellular signal intensities. Raman spectroscopic measurements indicate that FM-PA predominantly accumulates in ester-rich regions, most likely corresponding to lipid droplets. Although FM-PA provides higher detection sensitivity due to its strong fluorescence signal, its practical applicability is constrained by reagent toxicity and photobleaching.

In contrast, RM analysis of dPA reveals deuterated regions not only within lipid droplets but also in other intracellular compartments, including the cytosol and the nucleus. This broader spatial distribution suggests that the measured dPA concentrations reflect widespread incorporation of the deuterated fatty acid throughout the cell, rather than confinement to lipid-storage organelles. Consequently, RM-based quantification of dPA provides a more comprehensive and physiologically relevant representation of intracellular fatty acid uptake and metabolism.

4. Quantitative analysis of local fatty acid concentration at the single-pixel level

Figure 6 illustrates the single-pixel–resolved distribution of dPA concentrations within representative individual cells following 6 h of incubation with 50 µM and 200 µM dPA. The pixel-level concentration maps and histograms reveal pronounced intracellular heterogeneity, with distinct regions exhibiting low, intermediate, and high dPA concentrations within the same cell and a pronounced dependence on the applied incubation dose of dPA in extracellular solution. This approach enables direct visualization of how dPA concentration is distributed at the level of individual pixels (1 µm) across single cells. As shown in **Figure 6**, the concentration range varies substantially with the dPA concentration used for cell incubations. For cells incubated for 6 hours with the lower dPA concentration (50 µM), the maximum pixel-level concentration reaches approximately 390 mM. In contrast, under the same incubation time but at the higher applied concentration (200 µM), the maximum pixel-level concentration increases dramatically, reaching nearly 1600 mM.

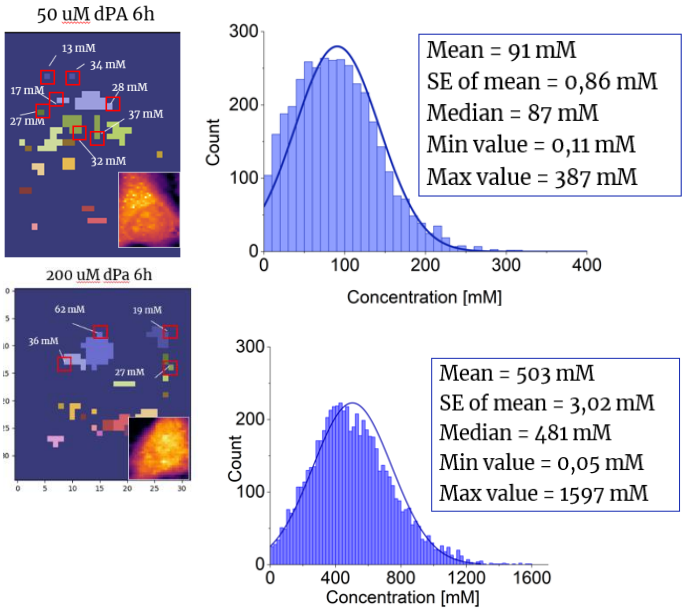

Figure 6. Single pixel distribution of concentrations of dPA analyzed in representative single cells after 6 h of incubation with 50 µM and 200 µM dPA.

In addition to the change in the upper concentration limit calculated at the single-pixel level, the mean pixel-level dPA concentration calculated across the entire cell population also shows a clear dose dependence, increasing substantially with higher incubation concentration. The average intracellular dPA concentration measured across the whole-cell population differed markedly from that in the incubation medium. For cells incubated with 50 µM dPA, the mean intracellular concentration was 91 mM; for cells incubated with 200 µM dPA, it increased to 503 mM. This indicates that elevated extracellular dPA levels not only promote the formation of highly enriched local regions but also increase the average intracellular dPA content. These findings underscore the pronounced heterogeneity of the mechanisms of datty acid uptake and metabolism in cells and highlight the importance of pixel-resolved analysis in Raman spectroscopy. In RM-based measurements, spectra are acquired from a wide variety of intracellular locations, including distinct organelles and chemically diverse microenvironments. This intrinsic cellular complexity naturally leads to a broad distribution of measured concentration values. Consequently, single-pixel analysis provides critical insight into the spatial variability of dPA accumulation that would be obscured by averaging approaches at the whole-cell or subcellular level.

Conclusion

In this study, we present a comprehensive, multi-scale framework for the quantitative determination of intracellular fatty acid concentrations using labelled palmitic acid, combined with RM (dPA) and FM (FL-PA). By integrating calibration-based RM with spatially resolved imaging, we establish a robust methodology capable of quantifying fatty acid concentrations across multiple

biological length scales, from entire single cells to selected subcellular regions and down to individual pixels. This approach addresses a critical gap in lipidomics, in which conventional techniques typically yield bulk or averaged measurements and lack spatial specificity. A key outcome of this work is the demonstration that intracellular concentrations of fatty acids can significantly exceed their extracellular incubation levels. Despite the use of micromolar concentrations of dPA in the culture medium, Raman-based quantification revealed apparent intracellular concentrations reaching the millimolar range, particularly within lipid-rich compartments. This discrepancy underscores the importance of local concentration measurements and highlights the limitations of interpreting cellular lipid uptake solely based on applied extracellular doses or total cellular content.

The single-cell analysis provides a global overview of fatty acid uptake and metabolic incorporation, revealing clear time- and dose-dependent trends in fatty acid incubation in cells. At short incubation times, intracellular dPA concentrations were largely independent of the applied dose, suggesting saturation or kinetic limitations of uptake and early metabolic processing. With prolonged incubation, however, a strong dose dependence emerged, indicating continued accumulation and intracellular retention of deuterated fatty acids. These findings emphasize that incubation time is a critical parameter in studies of lipid uptake and metabolism and must be carefully controlled and reported. Moving beyond whole-cell averaging, selected-area analysis highlights the pronounced spatial heterogeneity in fatty acid distribution within cells. Raman spectroscopy revealed that deuterium-rich regions are not uniformly distributed but instead localized within chemically distinct subcellular domains. Comparison using FM showed that FM-PA preferentially accumulates in ester-rich regions, most likely lipid droplets, whereas dPA detected by Raman spectroscopy is distributed more broadly throughout the cell, including the cytosol and nucleus. These differences reflect the distinct physicochemical properties, toxicity, and intracellular behavior of the two probes and illustrate the limitations of fluorescence-based approaches for quantitative lipid analysis. The single-pixel analysis is the most powerful approach of the presented methodology, enabling local quantification of fatty acid concentration with submicrometer spatial resolution. This approach revealed extreme heterogeneity in dPA distribution, with pixel-level concentrations spanning more than an order of magnitude within the same cell population. Significantly, the maximum local concentration increased substantially with higher incubation doses, reaching values that were substantially higher than those observed under lower-dose conditions. Such heterogeneity would be entirely obscured by averaging approaches, underscoring the necessity of pixel-resolved chemical mapping for accurate interpretation of intracellular lipid dynamics.

Collectively, these results demonstrate that Raman microscopy, when combined with rigorous calibration and appropriate segmentation strategies, enables quantitative, spatially resolved analysis of fatty acid uptake and metabolism in intact cells. Unlike FM, Raman-based detection of deuterated probes is non-destructive and applicable at physiologically relevant concentrations without introducing significant cytotoxicity. This makes Raman spectroscopy particularly well-suited to studying lipid transport, storage, and metabolic fluxes in complex biological systems.

The methodology presented here has broad implications for the study of lipid biology, including investigations of lipotoxicity, metabolic adaptation, and cancer cell metabolism, where local lipid concentrations play a decisive role in cellular fate. By enabling direct measurement of fatty acid concentrations in specific cellular compartments, this approach provides a powerful tool for linking lipid distribution to function and pathology. Ultimately, multi-scale, quantitative Raman imaging represents a significant step toward spatially resolved lipidomics and fluxomics in living and fixed biological systems.

Acknowledgements

This research was funded by the National Science Center Poland (NCN), Maestro 2022/46/A/ST4/00054 to Malgorzata Baranska.

References

1. Han, J. & Kaufman, R. J. The role of ER stress in lipid metabolism and lipotoxicity. *J. Lipid Res.* **57**, 1329–1338 (2016).

2. Santos, C. R. & Schulze, A. Lipid metabolism in cancer. *FEBS J.* **279**, 2610–2623 (2012).
3. Borek-Dorosz, A. *et al.* From Single Molecular Detail to Subcellular Dynamics: Real-Time Kinetics Study of dPA Uptake with Raman-based Spectroscopy. *bioRxiv* 2025.11.21.689687 (2025) doi:10.1101/2025.11.21.689687.
4. Zhao, G. *et al.* Ovarian cancer cell fate regulation by the dynamics between saturated and unsaturated fatty acids. *Proc. Natl. Acad. Sci. U. S. A.* **119**, e2203480119 (2022).
5. Liu, R. *et al.* Lipid Metabolism Reprogramming in Cancer: Insights into Tumor Cells and Immune Cells Within the Tumor Microenvironment. *Biomed. 2025, Vol. 13,* **13**, (2025).
6. Hu, Y., Zhang, R. Q., Liu, S. L. & Wang, Z. G. In-situ quantification of lipids in live cells through imaging approaches. *Biosens. Bioelectron.* **240**, 115649 (2023).
7. Sharma, S. K. *et al.* An integrative Raman microscopy-based workflow for rapid in situ analysis of microalgal lipid bodies. *Biotechnol. Biofuels 2015 81* **8**, 164- (2015).
8. Du, J. *et al.* Raman-guided subcellular pharmaco-metabolomics for metastatic melanoma cells. *Nat. Commun. 2020 111* **11**, 1–16 (2020).
9. Zhou, Y., Xu, Y., Hou, X. & Xia, D. Raman analysis of lipids in cells: Current applications and future prospects. *J. Pharm. Anal.* **15**, 101136 (2025).
10. Nowakowska, A. M. *et al.* The Raman Map of the Human Cell. *Anal. Chem.* **97**, 16374–16382 (2025).
11. Klein, K. *et al.* Label-Free Live-Cell Imaging with Confocal Raman Microscopy. *Biophys. J.* **102**, 360–368 (2012).
12. Brazhe, N. A., Nikelshparg, E. I., Prats, C., Dela, F. & Sosnovtseva, O. Raman probing of lipids, proteins, and mitochondria in skeletal myocytes: a case study on obesity. *J. Raman Spectrosc.* **48**, 1158–1165 (2017).
13. Pacia, M. Z. *et al.* Estimation of the content of lipids composing endothelial lipid droplets based on Raman imaging. *Biochim. Biophys. Acta - Mol. Cell Biol. Lipids* **1865**, 158758 (2020).
14. Nahmad-Rohen, A. *et al.* Quantitative Label-Free Imaging of Lipid Domains in Single Bilayers by Hyperspectral Coherent Raman Scattering. *Anal. Chem.* **92**, 14657–14666 (2020).
15. Hamada, K. *et al.* Raman microscopy for dynamic molecular imaging of living cells. *https://doi.org/10.1117/1.2952192* **13**, 044027 (2008).
16. Greig, J. C., Tipping, W. J., Graham, D., Faulds, K. & Gould, G. W. New insights into lipid and fatty acid metabolism from Raman spectroscopy. *Analyst* **149**, 4789–4810 (2024).
17. Zhao, Z., Chen, C., Xiong, H., Ji, J. & Min, W. Metabolic Activity Phenotyping of Single Cells with Multiplexed Vibrational Probes. *Anal. Chem.* **92**, 9603–9612 (2020).
18. Jia, H. & Yue, S. Stimulated Raman Scattering Imaging Sheds New Light on Lipid Droplet Biology. *J. Phys. Chem. B* **127**, 2381–2394 (2023).
19. Manifold, B. & Fu, D. Quantitative Stimulated Raman Scattering Microscopy: Promises and Pitfalls. *Annu. Rev. Anal. Chem. (Palo Alto. Calif).* **15**, 269–289 (2022).
20. Li, M., Yang, L., Bai, Y. & Liu, H. Analytical Methods in Lipidomics and Their Applications. *Anal. Chem.* **86**, 161–175 (2013).
21. Pelletier, M. J. Quantitative analysis using Raman spectrometry. *Appl. Spectrosc.* **57**, (2003).
22. Potcoava, M. C., Futia, G. L., Gibson, E. A. & Schlaepfer, I. R. Lipid profiling using Raman and a modified support vector machine algorithm. *J. Raman Spectrosc.* **52**, 1910–1922 (2021).
23. Kumar, S. *et al.* Raman and infra-red microspectroscopy: towards quantitative evaluation for clinical research by ratiometric analysis. *Chem. Soc. Rev.* **45**, 1879–1900 (2016).
24. Kopec, M., Beton-Mysur, K. & Abramczyk, H. Raman imaging and chemometric methods in human normal bronchial and cancer lung cells: Raman biomarkers of lipid reprogramming. *Chem. Phys. Lipids* **257**, 105339 (2023).
25. Rensonnet, A. *et al.* Spectral fingerprinting of cellular lipid droplets using stimulated Raman scattering microscopy and chemometric analysis. *Analyst* **149**, 553–562 (2024).